Crystallization Kinetics and Melting Behavior of Poly[(trimethylene terephthalate)-*co*-(29 mol % ethylene terephthalate)] Copolyester

Ming Chen,[1] Chi-Yun Ko,[1] Hui-Chen Wang,[1] Ren-Yi Chen,[1] Chuan-Liang Wang,[1] Hsin-Ying Lu,[1] I-Min Tseng[2]

[1]*Institute of Materials Science and Engineering, National Sun Yat-Sen University, Kaohsiung 80424, Taiwan, Republic of China*
[2]*Material and Chemical Research Laboratories, Industrial Technology Research Institute, Hsinchu 300, Taiwan, Republic of China*

Received 14 April 2008; accepted 5 August 2008
DOI 10.1002/app.29671
Published online 17 February 2009 in Wiley InterScience (www.interscience.wiley.com).

ABSTRACT: The copolyester was characterized as having 71 mol % trimethylene terephthalate units and 29 mol % ethylene terephthalate units in a random sequence according to the NMR spectra. Differential scanning calorimeter (DSC) was used to investigate the isothermal crystallization kinetics in the temperature range (T_c) from 130 to 170°C. The melting behavior after isothermal crystallization was studied using DSC and temperature-modulated DSC by varying the T_c, the crystallization time, and the heating rate. The DSC thermograms and wide-angle X-ray diffraction patterns reveal that the complex melting behavior involves melting-recrystallization-remelting and different lamellar crystals. As the T_c increases, the contribution of recrystallization gradually falls and finally disappears. A Hoffman-Weeks linear plot yields an equilibrium melting temperature of 198.7°C. The kinetic analysis of the growth rates of spherulites and the change in the morphology from regular to banded spherulites indicate that a regime II→III transition occurs at 148°C. © 2009 Wiley Periodicals, Inc. J Appl Polym Sci 112: 2305–2314, 2009

Key words: polyesters; NMR; crystallization

INTRODUCTION

Poly(ethylene terephthalate) (PET) is a popular polyester, which is widely applied in fibers, films, bottles, and engineering thermoplastics. The multiple melting behavior of PET and its origin have been intensively studied.[1–12] However, PET crystallizes slowly.[13,14] When it is neat, it cannot be molded with acceptable molding cycles. Poly(trimethylene terephthalate) (PTT) is a relatively new commercialized polymeric material that crystallizes easily without the addition of nucleation agents.[15,16] For a long time, PTT did not find commercial interest because of the limited availability of 1,3-propanediol (3G), the monomer used for PTT synthesis. Recently, PTT has drawn attention because of Shell's break-through in lower-cost monomer processes.[17] Only limited information is available concerning its crystallization kinetics[17–22] and multiple melting behavior.[23–26]

Correspondence to: M. Chen (mingchen@mail.nsysu.edu.tw).

Contract grant sponsor: National Science Council of Taiwan, Republic of China; contract grant numbers: NSC 90-2216-E-110-014, 91-2216-E-110-010.

Modifications of the chemical composition and the sequence of comonomers in semicrystalline polymers by copolymerization alter both the crystallization kinetics and the morphology. Only a small number of studies on poly[(ethylene terephthalate)-*co*-(trimethylene terephthalate)] (PET/PTT) copolyesters have been published.[27–37] Most of these copolyesters were crystallizable, but some were amorphous depending on the compositions.[27–32] The composition of these copolyesters was determined only by ^{1}H-NMR.[27–32] Ponnusamy and Balakrishnan[28,29] synthesized a series of random PET/PTT copolyesters from dimethyl terephthalate (DMT), ethylene glycol (2G), and 3G by melt polycondensation techniques. A copolyester containing 71.0 mol % of 3G was found to have a molecular weight of 1612 g/mol and an intrinsic viscosity of 0.11 dL/g (solvent: *o*-chlorophenol at 30 ± 0.1°C). This copolyester was reported to be amorphous. Lee et al.[30] synthesized a series of PET/PTT copolyesters by reacting DMT, 2G, and 3G in a two-step reaction sequence. Thermal properties and nonisothermal crystallization kinetics of these copolyesters were examined by differential scanning calorimetry (DSC). Wu and Lin[31] investigated the isothermal crystallization kinetics and the melting behavior of PET/PTT copolyesters using DSC. They assumed that the distribution of

TABLE I
Typical Property Values[15,36–38]

	PTT-1	PT91/ET09	PT71/ET29	PT62/ET38
TT (mol %)	100	91.1	70.5	62.1
ET (mol %)	0	8.9	29.5	37.9
Number sequence length of TT	–	10.2	3.5	2.7
Number sequence length of ET	–	1.0	1.5	1.6
Randomness, B	0	1.10	0.97	0.99
[η] (dL/g) at 25°C	0.66[a]	0.84	0.70	0.70
T_m (°C)	224.1	216.6	185.7	171.3
T_m^0 (°C)	240.6	236.3	198.7	188.5
T_g (°C)	37.6	42.1	47.9	49.1
G' (× 10 μm/s) at $T_{G'}$	9.33	6.14	1.12	0.21
$T_{G'}$ (°C)	180	180	130	120
G'' (× 10^2 μm/s) at $T_{G''}$	0.50	6.10	2.05	0.28
$T_{G''}$ (°C)	218	207	166	160
$T_{II\rightarrow III}$ (°C)	205	196	148	135
Enthalpy of crystallization (J/g)	−55	−47	−35	−32
Absolute crystallinity (%)[b]	37.7	32.2	24.0	21.9

TT, trimethylene terephthalate; ET, ethylene terephthalate.
[a] At 37°C.
[b] Based on the heat of fusion for 100% crystalline PTT (146 J/g)

comonomers in these copolyesters was random, based on the fact that a single T_g value rather than two T_g values, which would correspond to possible blocks of PET and PTT.[30,31] Ko et al.[35] determined the compositions and the distribution of ethylene terephthalate (ET) and trimethylene terephthalate (TT) units from the quaternary aromatic carbons of a series of PET/PTT copolyesters. They investigated the melting behavior of copolyesters following nonisothermal crystallization using temperature-modulated DSC (TMDSC). Additionally, the isothermal growth rates of spherulites of PTT homopolymer,[15] PT91/ET09 (containing 9 mol % ET units),[36] and PT62/ET38[37] copolymers were measured. Crystallization kinetics and melting behaviors of them[15,36–38] were also investigated in detail. Their properties are tabulated in Table I.

The study reported here extends the current investigation on random copolyesters[35] and focuses on the crystallization kinetics and the melting behavior of PT71/ET29 (that is containing 29 mol % ET units) copolyester. ^{13}C-NMR was used to determine the composition and the comonomer distribution. In a wide range of isothermal crystallization temperature (T_c), DSC data were analyzed using the Avrami equation.[39,40] The linear growth rates of spherulites were measured using polarized light microscopy (PLM), and the regime transition temperature was determined from the Lauritzen-Hoffman (LH) equation.[41] The morphology of this copolyester at various T_c values was observed under PLM. Furthermore, the origin of the multiple melting behavior of isothermal crystallized specimens was elucidated using wide-angle X-ray diffraction (WAXD), DSC, and TMDSC by varying T_c, crystallization time, and heating rate. In the next part of PT71/ET29 copolyester, the regime transitions of I-II and II-III will be reported and further discussed.

EXPERIMENTAL

Materials and characterization

Developmental-grade PT71/ET29 copolyester was synthesized in three steps.[35,42] This copolyester had an intrinsic viscosity [η] of 0.70 dL/g measured in phenol/1,1,2,2-tetrachloroethane (3/2, w/w) at 25 ± 0.2°C. The ^{13}C-NMR and ^{1}H-NMR spectra of $CF_3COOD/CDCl_3$ (4/1, v/v) solutions were recorded on a Bruker AMX-400 NMR spectrometer at 320 K.

Copolyester pellets and the compressed sheets with a thickness of around 0.2 mm were dried at 45°C in a vacuum oven for 12 h to remove moisture before use. Amorphous specimen, quenched from the melt, was used to obtain its glass transition temperature (T_g) with a Perkin-Elmer Pyris 1 DSC at heating rates of 1, 5, and 10°C/min. The corresponding T_g at the zero heating rate was 47.9°C (321.0 K).

DSC measurements and sample preparation

A Perkin-Elmer Pyris 1 DSC was routinely calibrated with indium and zinc. About 3–5 mg of sample was used herein. In the isothermal crystallization study, the samples were initially heated up to 200°C at 10°C/min and held in the molten state for 5 min. They were then rapidly cooled to the predefined T_c between 130 and 170°C, and then crystallized (t_c) for three to five times the peak time to ensure complete

crystallization. After isothermal crystallization, the specimens were ready for DSC and WAXD studies. The specimens were scanned up to 220°C at 10 and 50°C/min, respectively, to study their melting behavior. The specimens were all treated under the same premelting conditions, except that the isothermal crystallization time was varied, to study the sequence of occurrence of the multiple melting peaks. They were then scanned directly from T_c up to 200°C at 50°C/min.

Measurements of TMDSC

The TMDSC measurements were performed on a TA Instruments Q100, equipped with a refrigerating system. The cell constant calibration was made using an indium standard, and the temperature calibration was conducted using indium and lead. A standard sapphire sample was used to measure the heat capacity calibration constant for the modulation study. Specimens in TA DSC sample pans were prepared isothermally in Pyris 1 DSC under the same conditions as described in the previous section. A heating rate of 3°C/min with a period of 40 s and a modulation amplitude of 0.318°C were chosen as a heating-only condition based on the specifications presented in the instrument manual.[43]

WAXD measurements

Specimens with a thickness of about 0.5 mm after complete isothermal crystallization at various T_c values were prepared using Pyris 1 DSC under the same conditions as described earlier. X-ray diffractograms at room temperature were obtained on a Siemens D5000 diffractometer with Ni-filtered Cu Kα radiation ($\lambda = 0.1542$ nm, 40 kV, 30 mA) at a scanning rate of 1°/min.

PLM measurements

The setups and the measurements for the experiments of PLM are described in previous studies.[44,45] Specimens were prepared by melting the PET/PTT samples on a slide glass at 220°C for 3 min. It was found that there was no difference between the measured growth rates after premolting at 200°C for 5 min or 220°C for 3 min.[15,46] The latter treatment was effective in reducing nucleation density to the point of allowing the measurement of spherulitic growth rate. The premolten specimens were rapidly cooled to a predefined temperature between 130 and 166°C. The development of the spherulites was recorded versus time during the crystallization. The optical character was determined using a primary red filter (λ-plate) located diagonally between the cross polarizers.

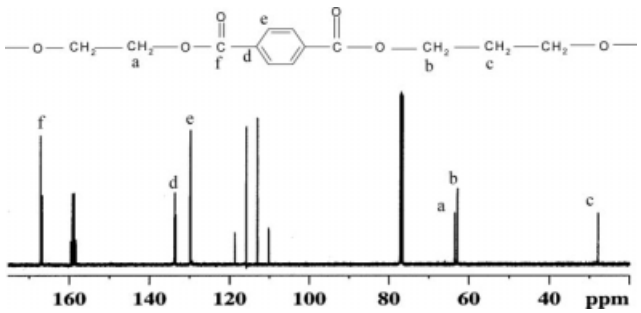

Figure 1 ^{13}C-NMR spectrum of the copolymer and its peak assignments.

RESULTS

Copolyester composition and sequence distribution

Figure 1 shows the ^{13}C-NMR spectrum of the copolymer and the peak assignments based on ^{13}C-NMR results obtained for PTT and PET homopolymers.[47] The three chemical shifts at 63.6, 62.9, and 28.0 ppm are associated with the ethylene carbons (label a) in the —OCH_2CH_2O— units and the methylene carbons α (label b) and β (label c) bonded to the ester oxygen in the —$OCH_2CH_2CH_2O$— units, respectively. The chemical shifts of the quaternary aromatic carbons (label d), the aryl carbons (label e), and the carbonyl carbons (label f) are at 133.6–134.0, 129.6–130.2, and 165.9–168.2 ppm, respectively. This copolyester is characterized as having 70.5 mol % TT units (P_{TT}) and 29.5 mol % ET units (P_{ET}), based on the analysis of quaternary aromatic carbons.[35] TT and ET units have average number sequence length of 3.5 and 1.5, respectively. The randomness B is given by $P(ETP)/(2P_{TT} \times P_{ET})$, where $P(ETP)$ is the probability of sequence ethylene-terephthalate-1,3 propylene (ETP, 40.3 mol% for this copolyester).[35] The B value is 0.97, which is within the experimental error, $B = 1.0$ for a random copolymer. For comparison, the composition was also determined from the ^{1}H-NMR integration area of the peak of the center methylene proton in the 3G moiety at 2.3 ppm to that of the methylene proton in the 2G moiety at 4.8 ppm.[30] The composition is 71.7 mol % TT units, which is very close to that observed in the ^{13}C-NMR spectrum. This copolyester was denoted as PT71/ET29 in an earlier article.[35]

Isothermal crystallization kinetics

The second column in Table II presents the isothermal crystallization time at temperatures ranging from 130 to 166°C by intervals of 4°C. The required time for full crystallization (t_c) increased from 27 min at 130°C to 150 min at 166°C. Columns 3 and 4 present the total enthalpy of crystallization (ΔH) and

TABLE II
Conditions and Kinetic Results of the Crystallization of Specimens Isothermally Crystallized in the Range 130–166°C

T_c (°C)	t_c (min)	ΔH (J/g)	$t_{1/2}$ (min)	n	k (min^{-n})
130	27	−34.9	3.3	2.24	4.11×10^{-6}
134	30	−34.8	3.5	2.31	3.95×10^{-6}
138	34	−33.6	3.6	2.34	4.04×10^{-6}
142	39	−34.4	4.3	2.33	1.99×10^{-6}
146	45	−34.3	5.1	2.35	1.07×10^{-6}
150	52	−35.1	6.4	2.34	8.38×10^{-7}
154	60	−37.3	8.2	2.36	6.05×10^{-7}
158	70	−36.4	9.0	2.36	3.02×10^{-7}
162	84	−35.8	15.1	2.38	5.41×10^{-8}
166	150	−33.6	28.8	2.41	2.31×10^{-8}

the half-time of crystallization ($t_{1/2}$). The average ΔH is -35 ± 1 J/g. The values of $t_{1/2}$ increased with T_c from 3.3 min at 130°C to 28.8 min at 166°C. The relative degree of crystallinity [$X_c(t)$] at time t was calculated. The Avrami plots of $\log[-\ln(1 - X_c(t))]$ vs. $\log t$ give the Avrami exponents and rate constants, n and k, which are presented in the last two columns: n increases from 2.2 to 2.4 while k decreases from 4.1×10^{-6} to 2.3×10^{-8} min^{-n} as T_c increases. Because of the slow isothermal crystallization, the values of ΔH and $X_c(t)$ at 170°C were not estimated.

Elucidating the melting behavior using conventional DSC

Figure 2 presents DSC thermograms at a heating rate of 50°C/min for specimens isothermally crystallized at 146 and 162°C for different time durations. Specimens crystallized at 146°C isothermally for 4 or ≥6 min yield double or triple melting peaks, respectively, in Figure 2(a). In Figure 2(b), specimens crystallized at 162°C isothermally for 10 min or ≥15 min yield a single melting peak or double melting peaks, respectively. The smallest induction times for the occurrence of the lower melting peak are about 6 and 15 min, respectively, for T_c values of 146 and 162°C. Figure 2(b) shows only one melting peak in a short crystallization time. These results reveal that the upper melting peaks appear first, and the lower melting peak occurs after further crystallization. In Figure 2, the peak location of the upper melting peaks remains constant over the full range of crystallization times.

Figures 3 and 4 present the DSC curves at heating rates of 10 and 50°C/min, respectively, for the specimens after complete crystallization at the indicated T_c. A small endothermic signal at 60–70°C is the T_g of semicrystalline specimens. Both heating curves show multiple endothermic peaks similar to those noted elsewhere.[30,31] However, a very broad and

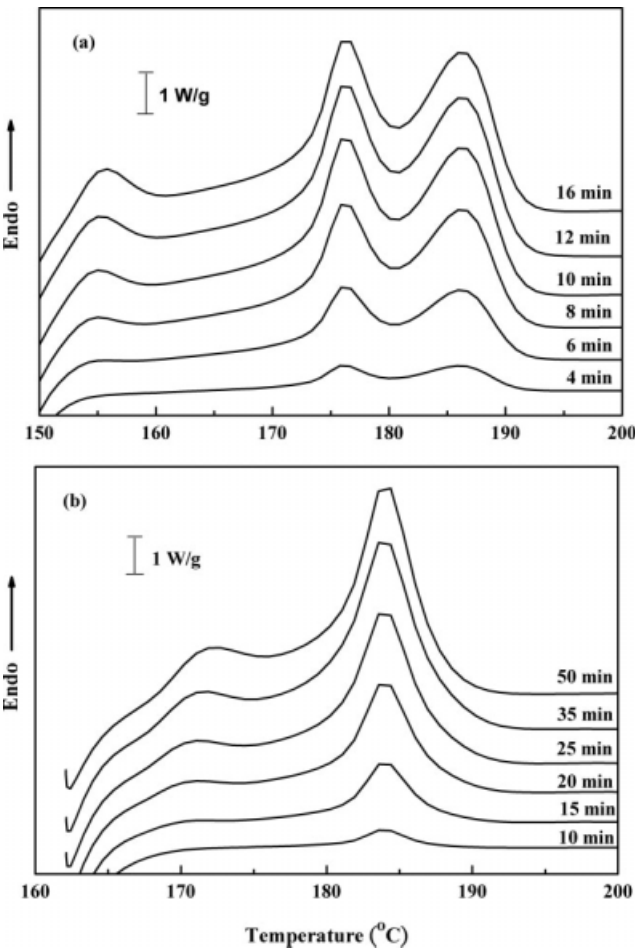

Figure 2 DSC thermograms at a heating rate of 50°C/min for specimens after premelting at 200°C for 5 min and then crystallized isothermally at (a) 146°C and (b) 162°C for various periods of time.

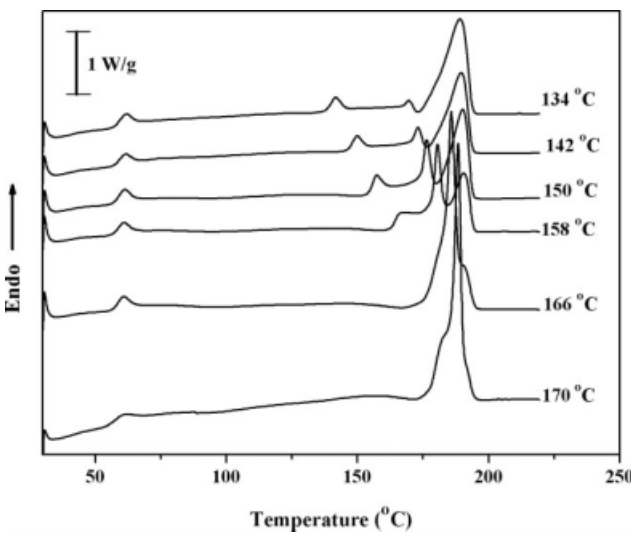

Figure 3 DSC thermograms at a heating rate of 10°C/min for specimens isothermally melt-crystallized at the temperatures indicated.

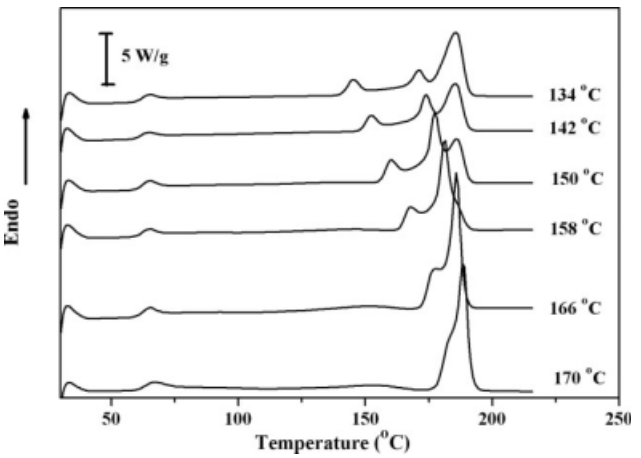

Figure 4 DSC thermograms at a heating rate of 50°C/min for specimens isothermally melt-crystallized at the temperatures indicated.

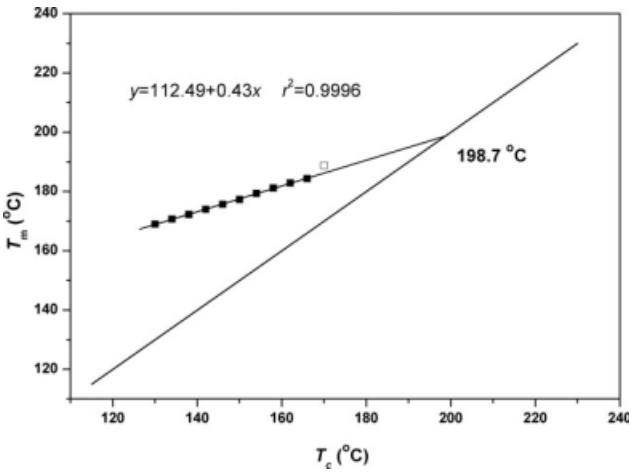

Figure 5 Hoffman-Weeks plot for determining the equilibrium melting temperature of the copolyester from conventional DSC data at a heating rate of 50°C/min.

weak endothermic peak was detected between T_g and the temperature of the followed peak. The reason is unclear. This smooth peak centers around 160°C, which is close to the melting temperature of PT50/ET50.[35] Table III presents the temperatures of the melting peaks after deconvolution for heating rates of 10 and 50°C/min. They are denoted as T_{I}, T_{II}, and T_{III} in the order of increasing temperature: T_{I} is about 10°C above T_c at 10°C/min, and 11°C above T_c at 50°C/min. The peak temperature of primary crystals[36,37] (T_{II}) measured at a heating rate of 50°C/min is designated as T_m. Figure 5 shows T_m as a function of T_c to determine the equilibrium melting temperature, T_m^0. A solid line is plotted where $T_c = T_m$. According to the Hoffman-Weeks approach,[48] the experimental data are extrapolated (based on the linear regression of the data points, plotted as filled symbols, for T_c ranging from 130 to 166°C) until they intersect with the solid line. The temperature of intersection is T_m^0, which yields a value of 198.7°C.

TABLE III
Melting Peak Temperatures (°C) at Two Heating Rates

	T_{peak} (°C) at 10°C/min			T_{peak} (°C) at 50°C/min		
T_c (°C)	T_{I}	T_{II}	T_{III}	T_{I}	T_{II}	T_{III}
130	138.1	167.9	188.9	141.4	169.0	184.9
134	141.8	169.5	189.0	145.6	170.7	185.7
138	149.3	173.0	189.7	148.9	172.3	185.7
142	149.8	173.0	189.5	152.3	174.0	185.7
146	153.7	174.7	189.7	156.4	175.7	185.7
150	157.3	176.4	190.0	159.8	177.3	185.7
154	161.9	178.2	190.0	164.0	179.0	185.7
158	167.5	180.8	190.3	168.2	181.5	185.7
162	181.6	183.4	191.1	174.8	184.9	–
166	180.4	185.9	191.5	177.3	185.7	–
170	182.4	188.4	–	183.2	188.2	–

Elucidating the melting behavior using TMDSC

The total curves of TMDSC traces in Figure 6 present three distinct melting peaks labeled P_{I}, $P_{\mathrm{II,endo}}$, and P_{III} with increasing temperatures, denoted as T_{I}, T_{IIendo}, and T_{III}. One small exothermic peak that appears just prior P_{III} for $T_c \leq 146$°C is labeled as $P_{\mathrm{II,exo}}$ with a peak temperature at T_{IIexo}. P_{I} shifts to the high-temperature region as T_c increases, and T_{I} is about 5–6°C above T_c. $P_{\mathrm{II,endo}}$ shifts slowly to higher temperature and its intensity increases with T_c. The position of P_{III} (or T_{III}) varies very slightly with T_c, however, its intensity decreases with an increase in T_c. The total enthalpies of melting of the three peaks are then summed up as follows: they increase from 33.0 to 41.3 J/g as T_c increases. The exothermic enthalpy decreases from −1.3 to −0.1 J/g

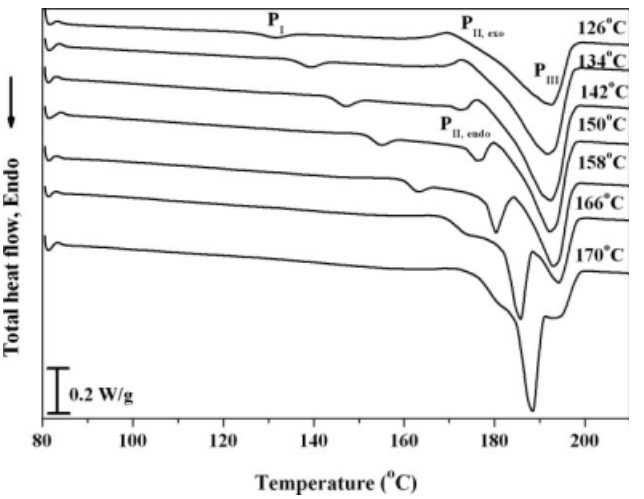

Figure 6 Total heat flow of TMDSC thermograms at a heating rate of 3°C/min for specimens isothermally melt-crystallized at the temperatures indicated.

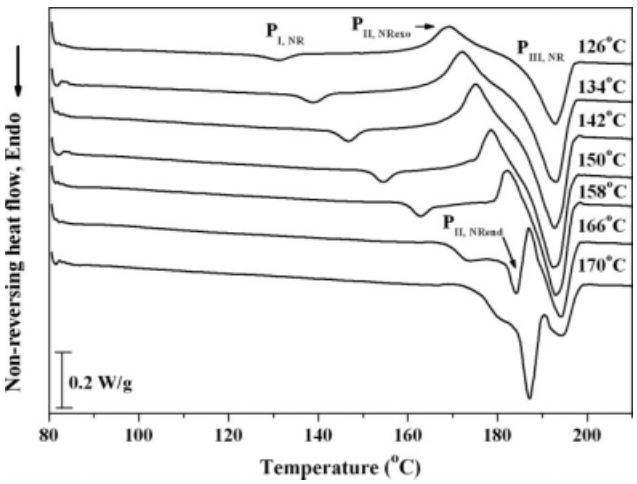

Figure 7 Nonreversible heat flow of TMDSC thermograms at a heating rate of 3°C/min for specimens isothermally melt-crystallized at the temperatures indicated.

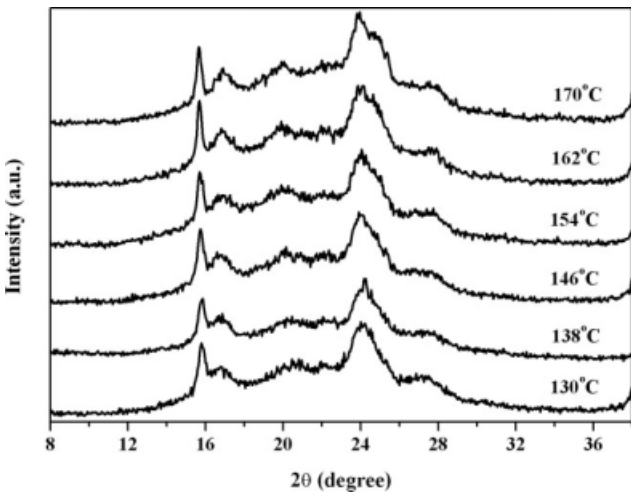

Figure 8 X-ray diffraction patterns of specimens isothermally crystallized at various temperatures.

as T_c increases from 122 to 138°C and is zero at $T_c \geq 142$°C.

TMDSC cannot discriminate quantitatively between reversible and nonreversible (NR) contributions of polymer melting.[49–51] A qualitative interpretation of NR curves is described later. NR curves (Fig. 7) show three endothermic melting peaks at $T_c > 158$°C, denoted as $P_{I,NR}$, $P_{II,NRendo}$, and $P_{III,NR}$, with increasing temperature. At $T_c < 170$°C, one crystallization exotherm is observed between the two melting endotherms. The exothermic enthalpy (ΔH_{exoNR}) decreases as T_c increases from 122 to 166°C and is zero at $T_c = 170$°C.

WAXD results

Figure 8 shows WAXD patterns of this copolyester after crystallization at various isothermal temperatures. All of the samples yield the same diffraction peaks over the entire range of temperature, indicating that there is only one crystalline form in all the samples crystallized isothermally between 130 and 170°C. The same pattern was obtained with low noise signal for thicker specimens.[35] These patterns have the similar diffraction peaks as PTT homopolymer with a triclinic unit cell.[26,52–56]

Kinetic analysis of the growth rates of spherulites

The growth rate (G) of spherulites was determined before their impingement by measuring the spherulitic radii from PLM micrographs obtained at successive intervals during isothermal crystallization.[44,45] Figure 9 plots the temperature dependence of the growth rate. The growth rates range from 11.15 $\times 10^{-2}$ μm/s at 130°C to 2.05 $\times 10^{-2}$ μm/s at 166°C. Error bars are also plotted in Figure 9 for each experimental point (or T_c). As expected, the decline in the radial growth rate with increasing T_c is confirmed in this temperature range. The measurable maximum growth rate of this copolyester is around 1/16 of the measurable maximum growth rate of PTT homopolymer.[15,16]

The regime analysis based on the LH model[41] is used to treat the growth rate data presented in Figure 9. Figure 10 plots $\log G + U^*/[2.303R(T_c - T_g + 30)]$ as a function of $1/(T_c \Delta T f)$, yielding the value of K_g (slope × 2.303) in each regime. U^* and T_∞ are the WLF (Williams-Landel-Ferry) energy term and the WLF temperature, respectively, $\Delta T = (T_m^0 - T_c)$ represents the undercooling, and f denotes a correction term of the order of unity, which is normally expressed as

$$f = 2T_c/(T_m^0 + T_c) \quad (1)$$

The regime analysis of the LH model was conducted using the following values: $U^* = 1500$ cal/

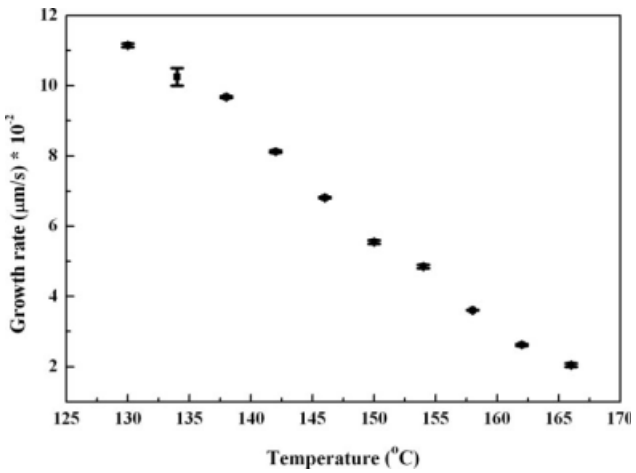

Figure 9 Variation of spherulitic growth rates with temperature.

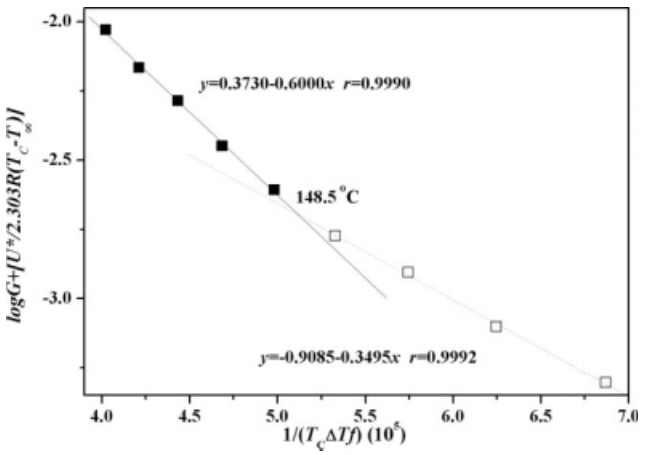

Figure 10 Kinetic analysis of the growth rate of spherulites. In this case, $U^* = 1500$ cal/mol, $T_\infty = T_g - 30$ K $= 291.0$ K and $T_m^0 = 471.8$ K.

mol, and $T_\infty = T_g - 30$ K with T_g at 321.0 K. $T_m^0 = 198.7°C = 471.8$ K was adopted. The two optimal fit lines correspond to the correlation coefficients (0.9990 and 0.9992), as shown in Figure 10. The break in the curve occurs at $T_c = 148.5°C$, and the ratio of the two slopes is 1.72. These results show that this sample exhibits a regime II→III transition at $\sim 148°C$.

Figures 11 and 12 present the photographs of the samples (between crossed polarizing plates), crystallized from the melt at various T_c. These spherulites exhibited typical negative birefringence, marked by a dark Maltese cross. Furthermore, a system of dark concentric rings was observed when the samples were crystallized at higher temperature, between 148 and 158°C (Fig. 12). These ringed images observed are similar to those of the morphology of banded spherulite, which is generally observed in crystalline polymers.[52] At lower temperatures of crystallization (130, 138, 146, and 147°C as presented in Fig. 11), the banded morphology disappears and a regular spherulitic image is obtained. PLM revealed a clear change in morphology (from 147 to 148°C). This temperature is very close to the regime II→III transition at 148.5°C, as determined from the kinetic analysis of the growth rates.

DISCUSSION

The occurrence of a single T_g at 60–70°C and a random parameter value of 0.97 indicate that the distribution of TT and ET units is statistically random. These units have number-average sequence lengths of 3.5 and 1.5, respectively. DSC results of isothermal crystallization between 130 and 166°C reveal that this PT71/ET29 copolyester has a heat of crystallization of -35 ± 1 J/g. The WAXD pattern also indicates that this copolyester is crystallizable. These results are different from those reported by Ponnusamy and Balakrishnan.[28,29] It might be due to the low molecular weight[28,29] and the premelting condition.[35]

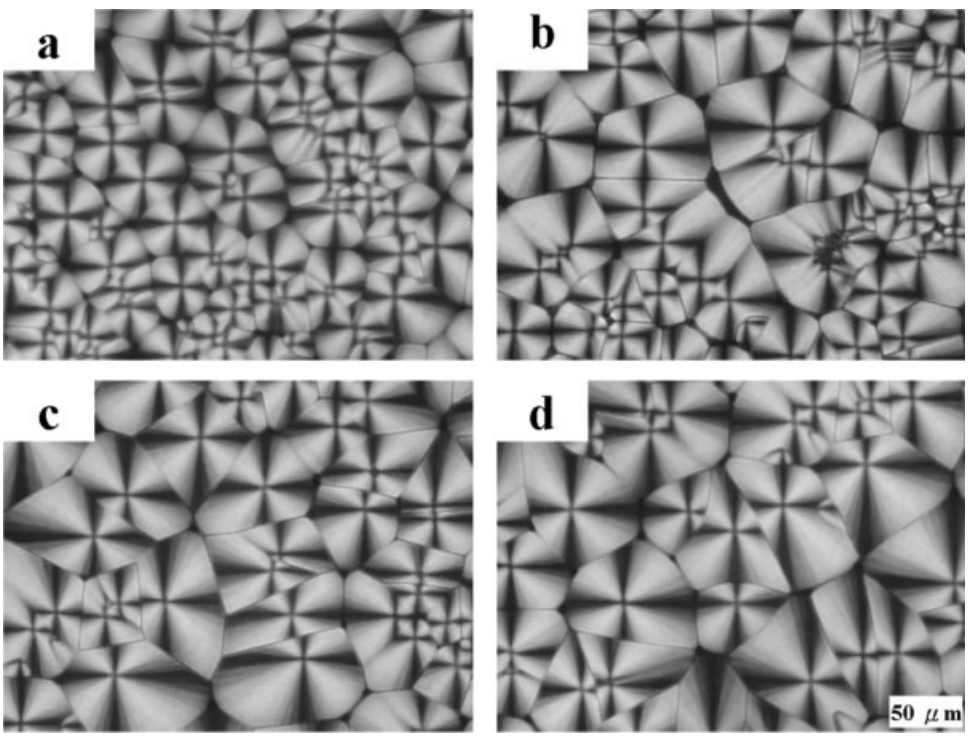

Figure 11 Transmission PLM micrographs with regular spherulites for specimens melt-crystallized at the indicated temperatures: (a) 130, (b) 138, (c) 146, and (d) 147°C.

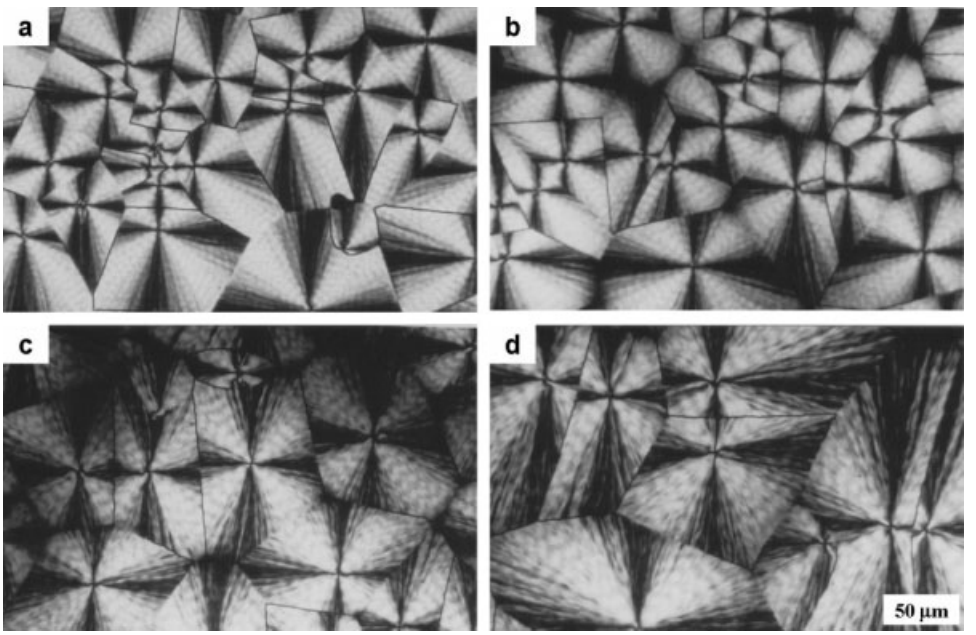

Figure 12 Transmission PLM micrographs with banded spherulites for specimens melt-crystallized at the indicated temperatures: (a) 148, (b) 150, (c) 154, and (d) 158°C.

Melting behavior and mechanism of multiple melting

As T_c increases from 134 to 170°C or when the heating rate increases from 3, 10, to 50°C/min, the general phenomena that are shown in Figures 3, 4, and 6 occur as follows. The peaks at T_I and T_{II} shift to higher temperature, and increase in intensity as T_c increases. This trend indicates that thicker crystalline lamellae develop as T_c increases. The position of the peak at T_{III} varies very little with T_c, but the intensity of the peak decreases as T_c increases. The ratio of intensities of the peak at T_{III} and that at T_{II} decreases as the heating rate increases, because less time is available for recrystallization since the heating rate is increased. These results show that the peak at T_{III} is related to the melting of the recrystallized crystals. The peak at T_{II} is associated with the fusion of the crystals that are grown during primary crystallization, and the peak at T_I is attributed to the final step, which is secondary crystallization. The distinctiveness of the peaks at T_I and T_{III} is ascribed to the slow growth rate of the primary crystals and the low crystallinity of this copolymer.[35–37]

In this study, only one crystal structure was formed, excluding the possibility of the presence of different crystal structures. Accordingly, the multiple melting peaks should be related to the melting of various lamellar crystals and/or recrystallized crystals. The isothermal crystallized specimens examined by TMDSC were prepared under the same conditions as used for conventional DSC. According to the NR curves (Fig. 7), the exothermic enthalpy (ΔH_{exoNR}) gives direct evidence of the melting-recrystallization-remelting behavior of PT71/ET29 copolyester. Exothermic recrystallization was not detected at $T_c = 170$°C because the growth rate of this copolyester was very low ($<2 \times 10^{-2}$ μm/s as in Table I). As T_c decreases, the melting temperature of the secondary crystals also decreases, and more time is available to recrystallize during the heating scan at a rate of 3°C/min. The crystallization exotherm is also assumed to be absent at $T_c = 170$°C in Figures 3 and 4 because less time is available for the recrystallization during heating at a rate of 10 or 50°C/min. However, in Figures 3, 4, and 6, an overlapped double or triple melting peaks are observed at $T_c = 170$°C. The absence of exothermic flow and the triple melting peaks support the mechanism, which involves various populations of lamellar crystals in the specimens that are isothermally crystallized over this temperature range. These results indicate that the complex melting behavior of this copolyester proceeds by both a melting-recrystallization-remelting mechanism and a mechanism that involves various lamellar crystals. As T_c increases, the contribution of melting-recrystallization-remelting process to the upper melting peak gradually decreases and finally disappears.

Melting peak temperatures and equilibrium melting temperature

Comparing the peak temperatures obtained at rates of 10 and 50°C/min at the same T_c reveals that T_I and T_{II} values at 50°C/min are in general higher than those at 10°C/min for $T_c \leq 158$°C (see Table

III). This result may follow from the superheating of the polymer at higher heating rate. The rise of T_{II} of the primary crystals is less than 1°C for $T_c \leq 158$°C. However, it becomes reduced and is 0.2°C less for $T_c \geq 166$°C. Conversely, T_{III} values obtained at 50°C/min are about 4°C less than those obtained at 10°C/min because the longer heating period at 10°C/min allows the specimens to recrystallize and/or reorganize during the heating scan. Figure 3 shows that at $T_c \leq 142$°C, the melting peak of primary crystals at T_{II} is much smaller than that at T_{III} as the heating rate is 10°C/min. Additionally, P_{II} is followed immediately by an exothermic behavior. T_{II} value for $T_c \leq 142$°C is not a true primary melting peak temperature when measured at a heating rate of 10°C/min. From the number of data points and the correlation coefficient values of linear regression, the results indicate that T_{II} measured at 50°C/min in this study maybe a better way to estimate T_m^0 without the superposition problem between the primary melting peak and the recrystallization exothermic peak. T_m^0 of 198.7°C, linearly extrapolated from the Hoffman-Weeks plot of the T_{II} values at a heating rate of 50°C/min, is used to estimate the regime transition temperature.

Wu and Lin[31] presented T_m^0 to be 197.6°C when PET/PTT copolyester containing 69 mol % TT units was heated at 10°C/min. Lee et al.[30] estimated T_m^0 to be 216.4 and 230.0°C for PET/PTT copolyesters that contain 60 and 78 mol % TT units, respectively. These T_m^0 values exceed the T_m^0 of the PT71/ET29 used in this study, and the T_m^0 used in Wu and Lin's article, even though they are all determined using the same Hoffman-Weeks plot method. In the work of Lee et al., all of the specimens were crystallized at T_c for 40 min, and then heated at a rate of 10°C/min. This isothermal time may be not long enough to complete the crystallization at most of the T_c according to Table II. Significant recrystallization is assumed to have occurred during the heating run at 10°C/min, based on the DSC thermograms in Figure 3 of the work of Lee et al. The overlap of the melting peak of the primary crystals at the lower temperature with the melting peak of the recrystallized crystals at the higher temperature may overestimate the peak temperature of the primary crystals, resulting in an overestimate of T_m^0.

Avrami exponent and regime transition temperature

In this study, n in the T_c range between 138 and 154°C is 2.3 ± 0.1, which fits very well with n of 2.3 ± 0.1 for T_c values between 139 and 154°C reported by Wu and Lin.[31] However, in that study the value of ΔH is between 16 and 22 J/g, which is much less than 35 ± 1 J/g measured in this study. In this study, the premelting condition for isothermal crystallization was held for 5 min at 200°C, which is higher than T_m^0 that was linearly extrapolated in Figure 5. The values of n are less than three, because, first, the thickness of the samples in the DSC studies is around 0.2 mm. At higher T_c values, the nucleation density is low and the diameter of the spherulites is about 0.1 mm. Hence, the growth of the spherulites was limited in two-dimensional spaces during the later stage of isothermal crystallization. Then, the homogeneous nucleation rate increases at low T_c, representing an athermal nucleation process that is followed by three-dimensional crystal growth in the early stage of isothermal crystallization. Finally, the cooling rate of the coolant system is not sufficiently high to avoid crystallization of this copolyester before cooling to a lower T_c.

PT71/ET29 copolyester showed a regime II→III transition at about 148°C, which was based on the LH kinetic analysis of the growth rates over the temperature range from 130 to 166°C. Wu and Lin[31] also measured the growth rates of spherulites. The regime transition was not found because only six data ranging from 139 to 154°C were used to do the kinetic analysis in that study.

CONCLUSION

The PET/PTT copolyester used had 71 mol % TT units and 29 mol % ET units. The value of the random parameter, 0.97, is close to 1.0 for a random copolymer. The average number sequence lengths of TT and ET units are 3.5 and 1.5, respectively. A single T_g value also suggests that this copolymer is a random copolyester. WAXD patterns suggest that there is only one crystal structure formed isothermally between 130 and 170°C. Conventional DSC and TMDSC curves showed triple melting peaks. The melting behavior revealed that primary crystals form before secondary crystals. A melting peak that follows the melting of primary crystals is related to the melting of the crystals that are recrystallized during the DSC heating scan. The exothermic behavior revealed by the TMDSC curves gives direct evidence of recrystallization. At $T_c = 170$°C, the absence of exothermic flow and the appearance of triple-melting peaks support the mechanism that involves various lamellar crystals. As T_c increases, the contribution of recrystallization gradually decreases and finally to zero.

Isothermal crystallization indicated that the values of the Avrami exponent were 2.3 ± 0.1. The Hoffman-Weeks linear plot gave an equilibrium melting temperature of 198.7°C. The kinetic analysis of the growth rates of the spherulites indicated a regime II→III transition at 148.5°C. A clear morphological change from regular negative spherulites to banded

negative spherulites was observed at 148°C in PLM micrographs. This temperature is consistent with the regime II→III transition, as determined from the kinetic analysis.

References

1. Roberts, R. C. Polymer 1969, 10, 117.
2. Roberts, R. C. J Polym Sci Part B: Polym Lett 1970, 8, 381.
3. Nealy, D. L.; Davis, T. G.; Kibler, C. J. J Polym Sci Part A-2: Polym Phys 1970, 8, 2141.
4. Holdsworth, P. J.; Turner-Jones, A. Polymer 1971, 12, 195.
5. Groeninckx, G.; Reynaers, H. J Polym Sci Polym Phys Ed 1980, 18, 1325.
6. Medellín-Rodríguez, F. J.; Phillips, P. J. Macromolecules 1996, 29, 7491.
7. Medellín-Rodríguez, F. J.; Phillips, P. J.; Lin, J. S.; Campos, R. J Polym Sci Part B: Polym Phys 1997, 35, 1757.
8. Qiu, G.; Tang, Z. L.; Huang, N. X.; Gerking, L. J Appl Polym Sci 1998, 69, 729.
9. Zhou, C.; Clough, S. B. Polym Eng Sci 1988, 28, 65.
10. Wang, Z. G.; Hsiao, B. S.; Sauer, B. B.; Kampert, W. G. Polymer 1999, 40, 4615.
11. Wang, Y.; Lu, J.; Shen, D. Polym J 2000, 32, 560.
12. Kong, Y.; Hay, J. N. Polymer 2003, 44, 623.
13. Wunderlich, B. Macromolecular Physics; Academic Press: New York, 1976; Vol. 2, p 163.
14. Jog, J. P. J Macromol Sci Rev Macromol Chem Phys 1995, C 35, 531.
15. Chen, C. C.; Chen, M.; Tseng, I. M. J Macromol Sci Phys 2002, B 41, 1043.
16. Chen, M.; Chen, C. C.; Ke, K. Z.; Ho, R. M. J Macromol Sci Phys 2002, B41, 1063.
17. Chuah, H. H. Polym Eng Sci 2001, B 41, 308.
18. Lee, K. M.; Kim, K. J.; Kim, Y. H. Polymer (Korea) 1999, 23, 56 (in Korean).
19. Huang, J. M.; Chang, F. C. J Polym Sci Part B: Polym Phys 2000, 38, 934.
20. Chisholm, B. J.; Zimmer, J. G. J Appl Polym Sci 2000, 76, 1296.
21. Wang, X. S.; Yan, D.; Tian, G. H.; Li, X. G. Polym Eng Sci 2001, 41, 1655.
22. Hong, P. D.; Chung, W. T.; Hsu, C. F. Polymer 2002, 43, 3335.
23. Pyda, M.; Wunderlich, B. J Polym Sci Part B: Polym Phys 2000, 38, 622.
24. Chung, W. T.; Yeh, W. J.; Hong, P. D. J Appl Polym Sci 2002, 83, 2426.
25. Wu, P. L.; Woo, E. M. J Polym Sci Part B: Polym Phys 2003, 41, 80.
26. Srimoaon, P.; Dangseeyun, N.; Supaphol, P. Eur Polym J 2004, 40, 599.
27. Smith, J. G.; Kibler, C. J.; Sublett, B. J. J Polym Sci Part A-1: Polym Chem 1966, 4, 1851.
28. Ponnusamy, E.; Balakrishnan, T. J Macromol Sci Chem 1985, A 22, 373.
29. Ponnusamy, E.; Balakrishnan, T. Polym J 1985, 17, 473.
30. Lee, J. W.; Lee, S. W.; Lee, B.; Ree, M. Macromol Chem Phys 2001, 202, 3072.
31. Wu, T. M.; Lin, Y. W. J Polym Sci Part B: Polym Phys 2004, 42, 4255.
32. Wei, G. F.; Wang, L. Y.; Chen, G. K.; Gu, L. X. J Appl Polym Sci 2006, 100, 1511.
33. Kiyotsukuri, T.; Masuda, T.; Tsutsumi, N. Polymer 1994, 35, 1274.
34. Shyr, T. W.; Lo, C. M.; Ye, S. R. Polymer 2005, 46, 5284.
35. Ko, C.-Y.; Chen, M.; Wang, H.-C.; Tseng, I.-M. Polymer 2005, 46, 8752.
36. Ko, C.-Y.; Chen, M.; Wang, C.-L.; Wang, H.-C.; Chen, R.-Y.; Tseng, I.-M. Polymer 2007, 48, 2415.
37. Chen, M.; Wang, H.-C.; Ko, C.-Y.; Chen, R.-Y.; Wang, C.-L.; Tseng, I.-M. Polym Int 2008, 57, 297.
38. Huang TW. MSc Thesis, National Sun Yat-Sen University, Kaohsiung, Taiwan, 2002.
39. Avrami, M. J Chem Phys 1939, 8, 212.
40. Avrami, M. J Chem Phys 1941, 9, 177.
41. Hoffman, J. D.; Davis, G. T.; Lauritzen, J. I., Jr.; In Treatise on Solid State Chemistry; Hannay, N. B., Ed.; Plenum Press: New York, 1976; Vol. 3, Chapter 7.
42. Tseng, I. M.; Kuo T. Y.; Shu W. C.; Huang, J. C. U.S. Pat.6,187,900 (2001).
43. TA Instruments. DSC 2910 Differential Scanning Calorimeter, Operator's Manual, Rev.8; TA Instruments: New Castle, Delaware, 1997; p C-73.
44. Chen, M.; Chen, J.-Y. J Polym Sci Part B: Polym Phys 1998, 36, 1335.
45. Chen, M.; Chung, C.-T. J Polym Sci Part B: Polym Phys 1998, 36, 2393.
46. Wei, G. F.; Hua, D. B.; Gu, L. X. J Appl Polym Sci 2006, 101, 3330.
47. Chen, M.; Wang, H. C.; Ko, C. Y. Abstr Pap Am Chem Soc 2002, 224, 166 Poly Part 2.
48. Hoffman, J. D.; Weeks, J. J. J Res Natl Bur Stand 1962, 66A, 13.
49. Wurm, A.; Schick, C. Colloid Polym Sci 2003, 281, 113.
50. Di Lorenzo, M. L.; Wunderlich, B. Thermochim Acta 2003, 405, 255.
51. Wunderlich, B. Prog Polym Sci 2003, 28, 383.
52. Ho, R. M.; Ke, K. Z.; Chen, M. Macromolecules 2000, 33, 7529.
53. Wang, B.; Li, C. Y.; Hanzlicek, J.; Cheng, S. Z. D.; Geil, P. H.; Grebowicz, J.; Ho, R. M. Polymer 2001, 42, 7171.
54. Poulin-Dandurand, S.; Pérez, S.; Revol, J. F.; Brisse, F. Polymer 1979, 20, 419.
55. Moss, B.; Dorset, D. L. J Polym Sci Polym Phys Ed 1982, 20, 1789.
56. Dorset, D. L.; Moss, B. In Polymer Characterization; American Chemical Society: Washington, DC, 1983; Chapter 22, p 409.